BNL-229299-2025-TECH
EIC-ADD-TN-157

Study of Quadrupole Fringe Fields in the Interaction Region of the Hadron Storage Ring of the Electron Ion Collider

F. Willeke

December 2025

Electron-Ion Collider

Brookhaven National Laboratory

U.S. Department of Energy

USDOE Office of Science (SC), Nuclear Physics (NP)

DISCLAIMER

Study of Quadrupole Fringe Fields in the Interaction Region of the Hadron Storage Ring of the Electron Ion Collider

F. Willeke, December 2025

1. Introduction

Fringe fields in quadrupole magnets are usually neglected in studies of beam dynamics at accelerators. However, the extreme optical parameters present in the final focus of a collider such as the Electron–Ion Collider (EIC) may give rise to effects that should not be overlooked.

The calculation of quadrupole fringe fields presented in this study follows the procedure outlined in Ref. [1], specialized to the case of a straight reference orbit (i.e., with no dipole field component). A right-handed Cartesian coordinate system is employed, with the z-axis aligned with the quadrupole axis and x and y denoting the horizontal and vertical transverse coordinates, respectively. The magnetic quadrupole field gradient, $G = \partial B_y / \partial x$, transitions from its peak value inside the quadrupole—where it is nearly independent of the longitudinal coordinate z—to zero at some distance beyond the magnet edge. Consequently, $G$is treated as a function of z. The region over which this variation occurs is defined as the quadrupole fringe field region.

The study begins with the development of a description of the magnetic field in the fringe region using a power-series expansion in the transverse coordinates $x$and y, consistent with the longitudinally varying gradient. A model for the z-dependence of the gradient is then proposed and adjusted to reproduce magnetic field data obtained from three-dimensional field calculations. To evaluate the impact of the fringe fields on beam dynamics, the corresponding vector potential is derived and incorporated into a Hamiltonian formulation of particle motion.

The significance of the fringe fields is quantified by calculating the amplitude-dependent tune shift from the Hamiltonian. Using linear beam optics parameters of the Hadron Storage Ring (HSR) of the EIC, the tune shift due to the fringe fields of all quadrupole magnets in the IR-6 interaction region is evaluated. Finally, the resulting tune shifts are compared with those arising from other nonlinear field components present in the HSR.

2 Magnetic Field in the Fringe Region of a Quadrupole Magnet

The static magnetic field in a region where the current density is zero, can be described by the gradient of a scalar potential Φ(x,y,z):

$$\vec{B} = \vec{\nabla}\,\Phi(x, y, z) \tag{1}$$

subject to the condition

$$\vec{\nabla}\,\mathrm{B} = 0. \tag{2}$$

This constraint immediately implies that the scalar potential satisfies the Laplace equation

$$\Delta\Phi = 0. \tag{3}$$

To capture the detailed spatial structure of the field—especially its gradual longitudinal variation in the fringe region—the scalar potential $\Phi(x, y, z)$ is expanded as a power series in the transverse coordinates x and y, evaluated at each longitudinal position z along the straight reference trajectory through the magnet center:

$$\Phi(x, y, z) = \sum_{n+m>0}^{\infty} C_{n,m}(z)\, \frac{x^n y^m}{n!\, m!}. \tag{4}$$

This expansion expresses the magnetic field as a hierarchy of multipole components whose strengths evolve smoothly along the longitudinal axis.

Substitution of this series into the Laplace equation yields a recursion relation that tightly couples the longitudinal dependence of the expansion coefficients to their transverse order:

$$C_{n+2,m}(z) + C_{n,m+2}(z) + C''_{nm}(z) = 0 \tag{5}$$

where the prime denotes differentiation with respect to z.

The magnetic field itself follows directly from the gradient of the scalar potential,

$$\vec{B} = \vec{\nabla}\, \Phi(x, y, z) = \sum_{n+m>0}^{\infty} \begin{bmatrix} C_{n+1,m}(z) \\ C_{n,m+1}(z) \\ C'_{n,m}(z) \end{bmatrix} \frac{x^n y^m}{n!\, m!} \tag{6}$$

It is assumed that the dipole fields are zero and there are only fields with midplane symmetry:

$$C_{10} = B_x(0,0,z) = 0,\ C_{0,1} = B_y(0,0,z) = 0,\ \ C_{11} = G(z),\ \ C_{20} = 0,\ \ C_{02} = 0,\ \ C_{00} \equiv 0 \tag{7}$$

We also verify that $\vec{\nabla} \times \vec{B} = 0$

$$\begin{aligned} \frac{\partial B_x}{\partial y} &= \sum_{n+m>0}^{\infty} C_{n+1,m+1}(z) \cdot \frac{x^n y^m}{n!m!} = \frac{\partial B_y}{\partial x} = \sum_{n+m>0}^{\infty} C_{n+1,m+1}(z) \cdot \frac{x^n y^m}{n!m!}, \\ \frac{\partial B_z}{\partial y} &= \sum_{n+m>0}^{\infty} C'_{n,m+1}(z) \cdot \frac{x^n y^m}{n!m!} = \frac{\partial B_y}{\partial z} = \sum_{n+m>0}^{\infty} C'_{n,m+1}(z) \cdot \frac{x^n y^m}{n!m!}, \\ \frac{\partial B_x}{\partial z} &= \sum_{n+m>0}^{\infty} C'_{n+1,m}(z) \cdot \frac{x^n y^m}{n!m!} = \frac{\partial B_z}{\partial x} = \sum_{n+m>0}^{\infty} C'_{n+1,m}(z) \cdot \frac{x^n y^m}{n!m!} \quad . \end{aligned} \tag{8a, b, c}$$

One identifies the coefficients C_{nm} as

$$C_{n,1} = \frac{\partial^n B_y}{\partial x^n}, \qquad C_{1,m} = \frac{\partial^m B_x}{\partial y^m}, \qquad C_{n+1,0} = \frac{\partial^n B_x}{\partial x^n},\ \ C_{0,m+1} = \frac{\partial^m B_y}{\partial y^m} \tag{9}$$

In particular, there is

$$C_{1,1}(z) = \frac{\partial B_y(x = 0, y = 0, z)}{\partial x} = \frac{\partial B_x(0,0,z)}{\partial y} = G(z). \tag{10}$$

Having this in mind, one can construct the power series for the magnetic field in the fringe field region: Using the recursion relation, equation (5) we put

$$-C''_{1,1} = C_{3,1} + C_{1,3}. \tag{11}$$

By preserving x-y symmetry of the quadrupole field, $B_x(\mathrm{x,y}) = B_y(y, x)$, we obtain

$$C_{3,1} = C_{1,3} = -\frac{1}{2}\cdot C''_{1,1} = -\frac{1}{2}\cdot G'' \tag{12}$$

The symmetry argument is used also to determine the next order coefficients by employing the recursion relation equation (4):

$$\begin{aligned} -C''_{3,1} &= \frac{1}{2}\cdot G'''' = C_{5,1} + C_{3,3} \\ -C''_{1,3} &= \frac{1}{2}\cdot G'''' = C_{3,3} + C_{1,5} \\ 0 &= C_{5,1} - C_{1,5} \\ C_{5,1} &= C_{33} \\ C_{5,1} &= C_{3,3} = \frac{1}{2}G'''' \end{aligned} \tag{13a,b,c}$$

This results in the following expressions for the transverse magnetic field in the fringe field region up to 5th order in the coordinates:

$$\begin{aligned} B_x &= G(z)\cdot y - \frac{G''}{12}\cdot(y^3 + 3x^2y) + \frac{1}{480}\cdot G''''\cdot(5x^4y + 10\cdot x^2y^3 + y^5) \\ B_y &= G(z)\cdot x - \frac{G''}{12}\cdot(x^3 + 3y^2x) + \frac{1}{480}\cdot G''''\cdot(5y^4x + 10\cdot x^3y^2 + x^5) \\ B_z &= G'\cdot(x\cdot y) - \frac{1}{12}\cdot G'''\cdot(x^3y + xy^3) \end{aligned} \tag{14a,b,c}$$

Note that this construction of the field implies $\nabla\vec{B} = 0$ and $\nabla\times\vec{B} = 0$

For the vector potential $\vec{A}$ that from which the magnetic field described by (equations 14) is derived by $\vec{B} = \vec{\nabla}\times\vec{A}$, a gauge field that preserves the symmetry in the x and y coordinates is chosen:

$$\vec{A} = \frac{1}{12}\cdot\begin{bmatrix} -\frac{G'}{12}\cdot(x^3 + 3y^2x) + \frac{1}{480}\cdot G'''\cdot(5y^4x + 10\cdot x^3y^2 + x^5) \\ \frac{G'}{12}\cdot(y^3 + 3x^2y) - \frac{1}{480}\cdot G'''\cdot(5x^4y + 10\cdot x^2y^3 + y^5) \\ \frac{1}{2}\cdot G(z)\cdot(y^2 - x^2) \end{bmatrix} \tag{15}$$

3 Fringe Fields of the Final Focus Quadrupoles in the Interaction Region for the Hadron Storage Ring of the EIC

The following is based on the 3D design of the EIC IR final focus quadrupole magnets. The quadrupole gradient on the design orbit in the fringe field region has been calculated using a numerical 3D field calculation [5] with appropriate magnet field calculation computer codes. Figure 1 shows the numerical data of the quadrupole field gradient G for $x = y = 0$ as a function of the pathlength of the straight design orbit z that passes through the center of the magnet.

Figure 1a shows the gradient over the entire magnet and Figure 1b shows only the fringe field region.

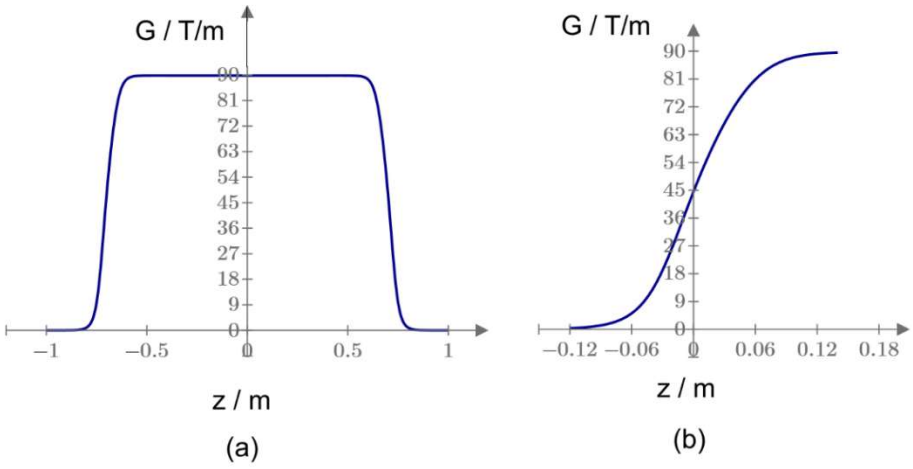

Figure 1: Results of the numerical magnetic field calculation for the quadrupole magnet Q1pf of the HSR in the EIC IR. Figure 1a shows the entire length of the magnet, Figure 1b shows only the fringe field region. (Curtesy Anis Ben Yaya see ref (5)). Note that the gradient is symmetric around the magnet longitudinal center.

The data in the fringe field region are modeled by an Enge-function [6], G_{model} as

$$G_{model}(z) = G_0 \cdot \frac{1}{1+exp\left(1+\sum_{n=1}^{4}\left(\frac{z-z_0}{\Delta_n}\right)^{2n}\right)} \tag{16}$$

and the parameters of this function are adjusted to minimize the mean square difference between the modeled function and the results of the numerical magnetic field calculation. The parameters are:

G_0 =332.14 T/m; z_0 =131.212 mm; Δ_1 =238.223 mm, Δ_2 =151.143 mm, Δ_3 =318.493 mm, Δ_4= 325.300 mm, z = z_0 corresponds to the hard edge position of the quadrupole.

The result of fitting G_{model} function is compared with the numerical data in Figures (2,3).

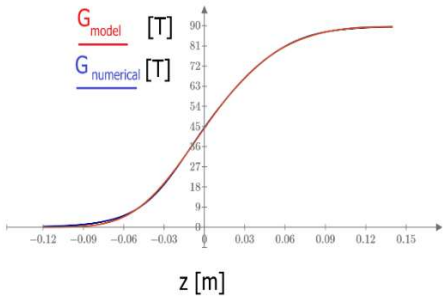

Figure 2: Comparison of numerical data with the model function of the quadrupole gradient of the magnet Q1pf in the fringe field region

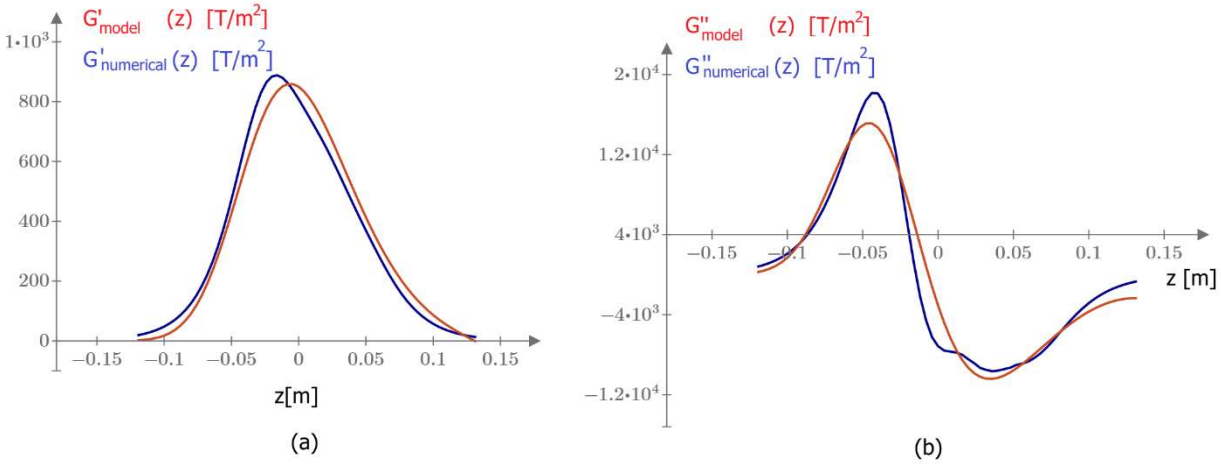

Figure 3 Comparison of the first (a) and second (b) derivative of the numerical and modeled quadrupole gradients G with respect to z in the fringe field region of quadrupole Q1pf.

Figures 1 and 2 show that the quadrupole gradient in the fringe field region is reasonably well described at a function of z by the model function G_{model}.

4 Beam Dynamics Assessment

The full assessment of the beam dynamics impact of the quadrupole fringe fields can only be evaluated by inserting the fringe field description in a particle tracking code. The purpose of this note, however, is to determine whether the impact of fringe fields is important compared to the other nonlinear fields in the accelerator. For this reason, in the following, the leading amplitude dependent tune shift (referred to as detuning term) is determined and compared with the tune shift resulting from sextupole magnets. The first step of the assessment is to write the Hamiltonian

$$H = \sqrt{m_0^2c^4 + c^2 \cdot (p_x - eA_x)^2 + c^2 \cdot (p_y - eA_y)^2 + c^2 \cdot (p_z - eA_z)^2} \tag{17}$$

(p_x, p_y, and p_z being the canonical momenta, and H = E = constant). In the usual accelerator coordinate system with the pathlength along z as the independent variable, the longitudinal momentum p_z becomes the Hamiltonian

$$p_z \equiv K = \sqrt{H^2 - m_0^2c^4 + c^2 \cdot (p_x - eA_x)^2 + c^2 \cdot (p_y - eA_y)^2} + eA_z \tag{18}$$

which leads to

$$K = P\sqrt{1 + c^2 \cdot (x' - \frac{eA_x}{P})^2 + c^2 \cdot (y' - \frac{eA_y}{P}eA_y)^2} + \frac{eA_z}{P}(18) \tag{19}$$

where $cP = \sqrt{H^2 - m_0^2 c^4}$ is the total mechanical momentum and $x', y' = \frac{p_{x,y}}{P}$.

Since all quantities under the square root besides 1 are small compared to unity, the square root is expanded to first order. Neglecting the constant term and using the vector potential of equation 15, we obtain the final form of K by limiting to leading terms (thus, terms of order >4 in the coordinates are neglected) for further analysis :

$$\mathrm{K} = -\frac{1}{2}x'^2 - \frac{1}{2}y'^2 - \frac{1}{2}\cdot\frac{e}{P}\cdot G(z)\cdot(y^2 - x^2) - \frac{1}{12}\frac{e}{P}\frac{\partial G(z)}{\partial z}(x^3x' + 3y^2xx' + y^3y' + 3x^2yy') \quad (20)$$

+higher order terms

The next step is expressing K in action J and angle Φ variables which removes the linear part

$$-\frac{1}{2}x'^2 - \frac{1}{2}x'^2 - \frac{1}{2}\cdot\frac{e}{P}\cdot G(z)\cdot(y^2 - x^2) \quad (21)$$

from K. Note that the linear optic uses the quadrupole strength inside the magnet and a quadrupole length that is obtained by integrating the gradient G(z) over z and dividing by the gradient inside the magnet. Thus, the quadrupole gradient component the fringe field is already taken into account in the linear optics in reasonable approximation.

Note also that there is a difference in the choice of angle variable: choosing $\Phi_{x,y} = \psi_{x,y}(z) + \phi_{x,y}$ adds the terms $Q_{x,y}\cdot J_{x,y}$ to the nonlinear part of the Hamiltonian, choosing $\Phi_{x,y} = \phi_{x,y}$, does not introduce this term. We will write just $\Phi_{x,y}$ for the sake of compactness but omit the terms Q·J as they are not important for the following.

The Hamiltonian now reads

$$\mathrm{K} = -\frac{1}{12}\frac{e}{P}\frac{\partial G(z)}{\partial z}(x^3x' + 3y^2xx' + y^3y' + 3x^2yy') + \text{higher order.} \quad (22)$$

Expressing the Hamiltonian K explicitly in the action and angle variables $J_{x,y}, \phi_{x,y}$ using

$$\begin{aligned} x &= \sqrt{2J_x\beta_x}\cos(\Phi_x), \quad y = \sqrt{2J_y\beta_y}\cos(\Phi_y) \\ x' &= -\sqrt{2J_x/\beta_x}(\alpha_x\cos(\Phi_x) + \mathrm{s}\,in(\Phi_x)), \\ y' &= -\sqrt{2J_y/\beta_y}(\alpha_y\cos(\Phi_y) + \mathrm{s}\,in(\Phi_y)) \end{aligned} \quad (23a,b,c,d)$$

($\beta_{x,y}$ are the lattice functions) and using

$$\kappa' = \frac{e}{P}\frac{\partial G(z)}{\partial z}, \quad (24)$$

one obtains

$$\mathrm{K} = \frac{1}{48}J_x^2\kappa'\beta_x\left\{\alpha_x\sum_{m=-4,-2}^{4}\frac{4!}{\frac{4-m}{2}!\frac{4+m}{2}!}e^{im\Phi_x} + \sin(\Phi_x)\sum_{m=-3,-1}^{3}\frac{3!}{\frac{3-m}{2}!\frac{3+m}{2}!}e^{im\Phi_x}\right\} + \frac{3}{48}J_xJ_y\kappa'\beta_y\cdot(1+\cos(2\Phi_y))\{\alpha_x(1+\cos(2\Phi_x)) + \sin(2\Phi_x)\} \quad (25)$$

$$+\frac{1}{48}J_y^2\kappa'\beta_y\left\{\alpha_y\sum_{m=-4,-2}^{4}\frac{4!}{\frac{4-m}{2}!\frac{4+m}{2}!}e^{im\Phi_y}+\sin(\Phi_y)\sum_{m=-3,-1}^{3}\frac{3!}{\frac{3-m}{2}!\frac{3+m}{2}!}e^{im\Phi_y}\right\}$$
$$+\frac{3}{48}J_xJ_y\kappa'\beta_x\cdot(1+\cos(2\Phi_x))\{\alpha_y(1+\cos(2\Phi_y))+\sin(2\Phi_y)\}$$
$$+\text{ higher order}$$

The amplitude dependent tune shift is obtained by expanding the Hamiltonian in Fourier series and retaining only 0^{th} order and terms that are independent on the phases $\Phi_{x,y}$ (corresponding to averaging the Hamiltonian over the phases) which implies integrating over the fringe field region which results in

$$\Delta Q_x(J_x,J_y)=\frac{1}{2\pi}\int\frac{<\partial K>}{\partial J_x}dz,\quad \Delta Q_y(J_x,J_y)=\frac{1}{2\pi}\int\frac{<\partial K>}{\partial J_y}dz \tag{26}$$

The phase averaging results in elimination of all the terms that have a phase dependence, and one is left with 'constant' terms:

$$<K>_{\phi_{x,y,z}}=\frac{1}{8\pi}\left(\beta_x\alpha_x\kappa'J_x^2+2\cdot(\beta_y\alpha_x+\beta_x\alpha_y)\cdot\kappa'J_xJ_y+\beta_y\alpha_y\kappa'J_y^2\right)$$
$$+\text{ higher order} \tag{27}$$

The amplitude dependent tune shift terms are obtained by integrating over the fringe field region $[-z_0,+z_0]$:

$$\Delta Q_x(J_x,J_y)=\frac{1}{4\pi}\int_{-z_0}^{z_0}\beta_x(z)\alpha_x(z)\kappa'(z)dz\cdot J_x+\frac{1}{4\pi}\int_{-z_0}^{z_0}\left(\beta_x(z)\alpha_y(z)+\beta_y\alpha_x\right)\cdot\kappa'(z)dz\cdot J_y \tag{28}$$
$$\Delta Qy(J_x,J_y)=\frac{1}{4\pi}\int_{-z_0}^{z_0}\beta_y(z)\alpha_y(z)\kappa'(z)dz\cdot J_y+\frac{1}{4\pi}\int_{-z_0}^{z_0}\left(\beta_x(z)\alpha_y(z)+\beta_y\alpha_x\right)\kappa'(z)dz\cdot J_x$$

Thus, the three detuning terms are

$$Q_{xx}=\frac{1}{4\pi}\int_{-z_0}^{z_0}\beta_x(z)\alpha_x(z)\kappa'(z)dz \tag{29a,b,c}$$
$$Q_{yy}=\frac{1}{4\pi}\int_{-z_0}^{z_0}\beta_y(z)\alpha_y(z)\kappa'(z)dz$$
$$Q_{xy}=\frac{1}{4\pi}\int_{-z_0}^{z_0}\left(\beta_x(z)\alpha_y(z)+\beta_y(z)\alpha_x(z)\right)\cdot\kappa'(z)dz$$

6 Evaluation of Detuning Terms

The beam optical functions are calculated using a hard-edge quadrupole model: constant gradient inside the quadrupole and zero gradient outside the hard edge. The error by using this model is small. Thus, the lattice functions outside the hard-edge border are given by:

$$\beta_{x,y}(z)=\beta_{x0,y0}-2\cdot\alpha_0\cdot(z-z_0)+(1+\alpha_0^2)\frac{(z-z_0)^2}{\beta_{x0,y0}} \tag{30}$$

where z_0 is the hard-edge position. Inside the quadrupole, the β-function is written using the quadrupole matrix and the generating trajectories

$$M_q(z) = \begin{bmatrix} \cos(\sqrt{-\kappa}z) & \frac{\sin(\sqrt{-\kappa}z)}{\sqrt{\kappa}} & 0 & 0 \\ -\sqrt{\kappa}\cdot\sin(\sqrt{-\kappa}z) & \cos(\sqrt{-\kappa}z) & 0 & 0 \\ 0 & 0 & \cosh(\sqrt{\kappa}z) & \frac{\sinh(\sqrt{\kappa}z)}{\sqrt{\kappa}} \\ 0 & 0 & \sqrt{\kappa}\cdot\sinh(\sqrt{\kappa}z) & \cosh(\sqrt{\kappa}z) \end{bmatrix} \tag{31}$$

$$\vec{u} = \begin{bmatrix} \sqrt{\beta_{x0}} \\ -\frac{\alpha_{x0}}{\sqrt{\beta_{x0}}} \\ \sqrt{\beta_{y0}} \\ -\frac{\alpha_{y0}}{\sqrt{\beta_{y0}}} \end{bmatrix} \qquad \vec{v} = \begin{bmatrix} 0 \\ \frac{1}{\sqrt{\beta_{x0}}} \\ 0 \\ \frac{1}{\sqrt{\beta_{y0}}} \end{bmatrix} \tag{32}$$

The parameter κ is the quadrupole strength $\frac{e}{P}\frac{\partial B_y}{\partial x}$. Equation (31) is the matrix for a horizontally focusing magnet. For a vertically focusing magnet, the hyperbolic and trigonometric functions are interchanged.

The lattice functions are then given by

$$\begin{aligned} \beta_{x,y}(z) &= \left(M_q(z)\cdot\vec{u}\right)_{0,2}^2 + \left(M_q(z)\cdot\vec{v}\right)_{0,2}^2 \quad (29a) \\ \alpha_{x,y}(z) &= \left(M_q(z)\cdot\vec{u}\right)_{0,2}\left(M_q(z)\cdot\vec{u}\right)_{1,3} + \left(M_q(z)\cdot\vec{v}\right)_{0,2}\left(M_q(z)\cdot\vec{v}\right)_{1,3} \end{aligned} \tag{33}$$

The lattice functions for the fringe field are calculated by using $\beta_x = 0.9\ m,\ \beta_y = 0.06\ m,$ $\alpha_x = 0, \alpha_y = 0$ in the interaction point IP-6 and by using the κ -value of the quadrupole Q1apf $\kappa = 0.0927\ m^{-2}$. The resulting lattice functions in the fringe field region are plotted in Figure 4.

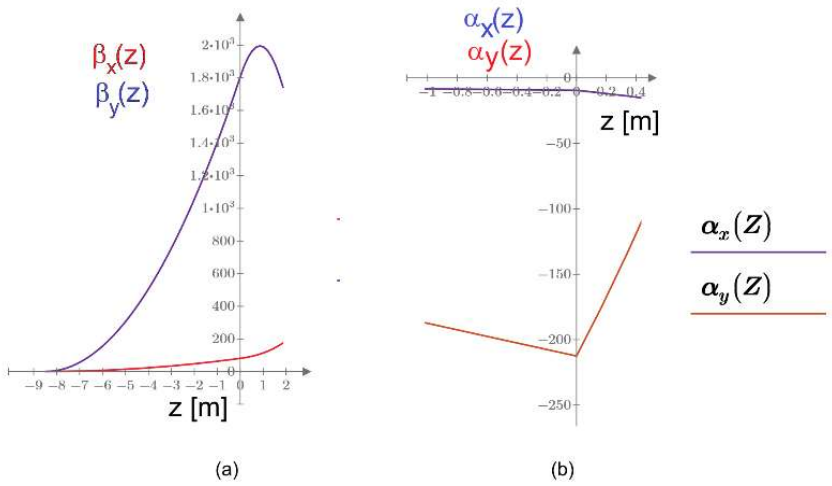

Figure 4: Lattice functions in the fringe field (IP side) of the HSR final focus quadrupole Q1apf. Note that the discontinuity of α' is due to the hard-edge optics model, an approximation which is expected to have only a minor impact.

With these parameters, the detuning values of the front end of Q1apf are obtained as

$$Q_{xx} = \frac{1}{4\pi}\int_{-z_0}^{z_0} \beta_x(z)\alpha_x(z)\kappa'(z)dz = 1.082 \cdot m^{-1} \qquad (34a,b,c)$$

$$Q_{yy} = \frac{1}{4\pi}\int_{-z_0}^{z_0} \beta_y(z)\alpha_y(z)\kappa'(z)dz = -296.01 \cdot m^{-1}$$

$$Q_{xy} = \frac{1}{4\pi}\int_{-z_0}^{z_0} \big(\beta_x(z)\alpha_y(z) + \beta_y(z)\alpha_x(z)\big)\kappa'(z)dz = 10.14 \cdot m^{-1}$$

The corresponding amplitude dependent tune change for a particle a an amplitude of 3 sigma of the beam size is $\Delta Q_x = 6.74 \cdot 10^{-6}$ and $\Delta Q_y = 2.038 \cdot 10^{-5}$. As there are 12 end fields of the final focus magnets in the IR, these numbers are not necessarily negligible, especially the Q_{yy} value. This requires a closer look at all the fringe fields in the IR region.

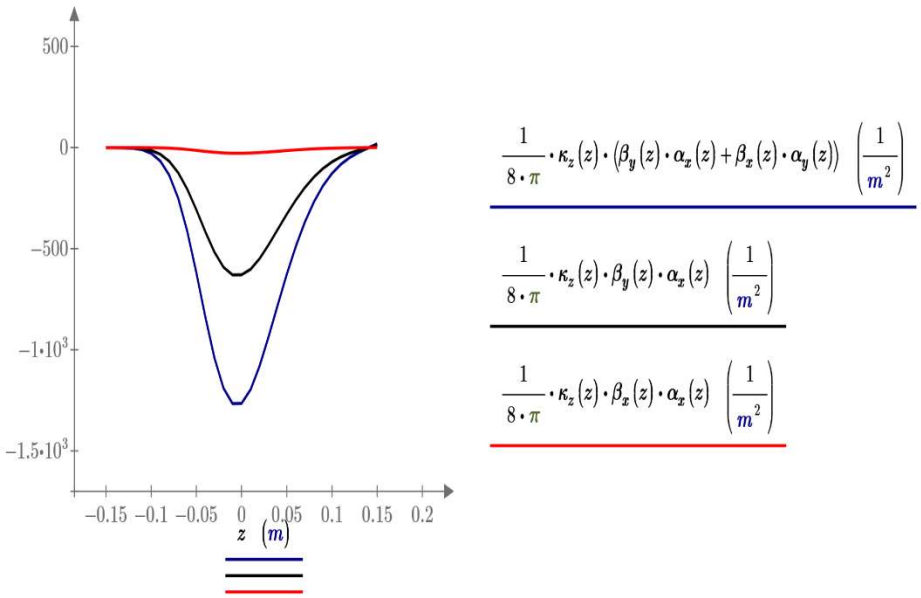

Figure 5: Sharply peaked integrands of the tuning terms Q_{xx}, Q_{yy}, and Q_{xy} according to equations 30a,b,c

As the sharply peaked shapes of the integrands for the detuning terms (see Figure 5) are due the z-dependent gradient $G'(z)$, and the lattice functions do not change strongly inside the fringe fields, a quasi-thin lens approximation is proposed. The integral 34b is divided by the peak values of the integrand

$$z_{eff} = \int_{-z_0}^{z_0} \frac{\beta_y(z)\alpha_y(z)\kappa'(z)dz}{\beta_y(0)\alpha_y(0)\kappa'(0)} = 1.1\ cm \tag{35}$$

and we obtain an effective fringe field width which turns out z_{eff} = 1.1 cm

This approximation is employed for a quick assessment of **the order of magnitude** of the contributions from all quadrupole end fields in the IR to the fringe-field driven detuning terms.

7 Relevant Beam Optical Parameters in IR6 and Evaluation of the Quadrupole Fringe Field Detuning

The table I below summarizes the contribution to the detuning terms from all HSR IR quadrupole. For each quadrupole there are two entries: the lattice function at the front and the ones on the rear site. Note that a change in aperture implies a longer fringe field region and a longer z_{eff}. But at the same time G' reduces as well and the product G'·z_{eff} is not expected to change. However, this is still a rather course approximation.

Table I: Summary of Approximate Detuning Term Contributions from all HSR Quadrupoles in the IR

NAME	L	KL	β_x	β_y	α_x	α_y	k	G'(0)/G	k'(0)	Qxx	Qxy	Qyy
	[m]	[m^{-1}]	[m]	[m]	[m]	[m]	[m^{-2}]	[1/m]	[m^{-3}]	[m^{-1}]	[m^{-1}]	[m^{-1}]
YI6_QD2-in	3.3916	0.10957	873.94	65.42	-109.68	4.86	0.03231	9.493	-0.307	25.7	0.8	-0.1
YI6_QD2	3.3916	0.10957	1300.06	56.01	0.01	-1.75	0.03231	9.4930	0.3067	0.0023	-0.6111	-0.0263
Q3PF-in	0.7500	0.00790	1300.14	168.87	-0.01	-3.34	0.01054	9.4930	-0.1001	0.0012	0.3807	0.0494
Q3PF	0.7500	0.00790	1292.46	174.94	10.23	-4.78	0.01054	9.4930	0.1001	1.1576	-0.3839	-0.0732
Q2PF-in	3.8000	0.14291	890.43	443.52	8.47	-7.68	0.03761	9.4930	-0.3570	-2.3561	0.9644	1.0649
Q2PF	3.8000	0.14291	445.83	815.54	86.54	-107.33	0.03761	9.4930	0.3570	12.0579	7.1031	-27.3544
Q1BPF-in	1.6100	-0.08443	379.11	903.89	79.80	-112.99	-0.05244	9.4930	0.4978	13.1840	12.7666	-44.5063
Q1BPF	1.6100	-0.08443	197.69	1153.24	37.94	-34.80	-0.05244	9.4930	-0.4978	-3.2686	-16.0704	17.4860
Q1APF-in	1.4600	-0.13225	168.43	1181.28	35.02	-35.22	-0.09058	9.4930	0.8599	4.4401	26.6767	-31.3131
Q1APF	1.4600	-0.13225	103.71	1059.70	12.12	113.06	-0.09058	9.4930	-0.8599	-0.9462	-18.4946	-90.1835
Q1APR-in	1.8000	-0.14774	35.91	390.21	-6.63	-73.61	-0.08208	9.4930	0.7791	-0.1623	-3.5661	-19.5905
Q1APR	1.8000	-0.14774	79.07	556.93	-19.44	-10.65	-0.08208	9.4930	-0.7791	1.0484	7.9585	4.0453
Q1BPR-in	1.4000	-0.11491	99.71	567.63	-21.84	-10.75	-0.08208	9.4930	0.7791	-1.4850	-9.1849	-4.1628
Q1BPR	1.4000	-0.11491	194.45	508.47	-49.43	50.72	-0.08208	9.4930	-0.7791	6.5547	10.4140	-17.5887
Q2PR-in	4.5000	0.12866	371.00	367.70	-68.28	43.13	0.02859	9.4930	-0.2714	6.0181	2.1633	-3.7675
Q2PR	4.5000	0.12866	806.93	192.54	-9.14	3.04	0.02859	9.4930	0.2714	-1.7517	0.1639	0.1388
Q3PR-in	1.5000	0.00897	1282.66	80.98	-11.55	1.82	0.00598	9.4930	-0.0567	0.7357	-0.0692	-0.0073
Q3PR	1.5000	0.00897	1300.05	76.70	0.01	1.05	0.00598	9.4930	0.0567	0.0004	0.0679	0.0040
Q4PR-in	1.5000	0.03931	1300.05	49.84	-0.01	0.61	0.02621	9.4930	-0.2488	0.0018	-0.1717	-0.0066
Q4PR	1.5000	0.03931	1224.90	51.01	49.12	-1.40	0.02621	9.4930	0.2488	13.1025	0.1720	-0.0156
Q5PR-in	1.5000	-0.08605	25.48	137.32	7.01	-2.63	-0.05737	9.4930	0.5446	0.0852	0.4272	-0.1722
Q5PR	1.5000	-0.08605	10.64	127.69	3.30	8.77	-0.05737	9.4930	-0.5446	-0.0167	-0.2454	-0.5337
YI6_TQ4-in	0.7500	0.03895	26.12	28.84	-5.31	4.07	0.05193	9.4930	-0.4930	0.0599	0.0202	-0.0507
YI6_TQ4	0.7500	0.03895	33.81	23.81	-4.83	2.70	0.05193	9.4930	0.4930	-0.0705	-0.0102	0.0278
SUM										74.1252	21.2561	-216.6213

The detuning terms due to sextupole magnets in the HSR lattice have been computed by Y. Luo (7). The numbers are:

$$\frac{\partial Q_x}{\partial J_x} = 545\ m^{-1} \qquad (37)$$
$$\frac{\partial Q_x}{\partial J_y} = -2697.40\ m^{-1}$$
$$\frac{\partial Q_y}{\partial J_y} = 158.64\ m^{-1}$$

And the tune shift parameters corresponding to 1 unit of 10^{-4} of octupole errors at 25 mm radius in all HSR arc dipoles are around 2000 m^{-1}[8].

From the detuning coefficients, the nonlinear tune shifts with amplitude are calculated according to equation (28) using for the HSR design values of $J_x = 6.25$ nm and $J_y = 0.63$ nm. They are presented in Table II. The tune shift values from fringe fields and sextupoles are in the same order of magnitude. The sextupole induced tune shift values are about one order of magnitude larger than the detuning terms due to the fringe field.

Table II Comparison of Amplitude Dependent Tunes caused by lattice sextupoles in the HSR and the quadruple fringe fields in the HSR IR quadrupole magnets

	Fringe Field Contribution	Sextupole Contribution
	$[10^{-5}]$	$[10^{-5}]$
ΔQ_x	0.048878955	0.6659
ΔQy	-0.133487447	1.7127528

8 Conclusions

The results in tables I and II are not threatening but they may not be negligible. The strength of the detuning suggests that the fringe fields should be considered in tracking calculation to ensure there is no problem, especially if the dynamic aperture is tight already without taking fringe field effects into account. The thin lenses that are derived in this document could be used in tracking calculations, but it would be more reliable to use analytic expression for the lattice function and integrate over the fringe field region.

9 Acknowledgement

The author would like to acknowledge the support from Scott Berg who provided the IR beam optics for hadrons and Anis Ben Yahia who made the magnetic field calculations available and Yun Luo who calculated the second order nonlinear tune shift due to sextupoles in the HSR and Henry Lovelace who provided the nonlinear tune shift due to octupole errors in the dipole in the HSR magnets.

References

[1] C.J. Gardner, The Vector Potential in Accelerator magnets, Particle Accelerators, 1991, Vol 35, pp.215-226
[2] S. Caspi, M. Helm, J.L. Laslett, '3D Field Harmonics', LBL-30313, March 1991.
[3] M. Bassetti, 'Analytical formulae for multipolar potentials', DA□NE Technical Note G-26,
[4] C. Biscari, Low Beta Quadrupole Fringing Field on Off-Axis Trajectory, AIP Conf. Proc. 344, 88–93 (1995) https://doi.org/10.1063/1.48972
[5] Anis Ben Yahia calculated the magnetic field and provided the data, private communications
[6] H. A. Enge, Focusing of Charged Particles, edited by A. Septier (Academic Press, New York, 1967), Vol. 2, pp. 203–264
[7] Yun Luo, private communications
[8] Henry Lovelace, communications